Synthesis and Characterization of Bi doped $BaTiO_3$ ceramic

A Dissertation Submitted in partial fulfillment
FOR THE DEGREE OF MASTER OF SCIENCE IN PHYSICS
Under Academic Autonomy

NATIONAL INSTITUTE OF TECHNOLOGY, ROURKELA

By

Dhiraj Kumar Rana

Under the Supervision of

Prof. S. Panigrahi

DEPARTMENT OF PHYSICS
NATIONAL INSTITUTE OF TECHNOLOGY
ROURKELA - 769008

NATIONAL INSTITUTE OF TECHNOLOGY
ROURKELA

CERTIFICATE

This is to certify that the thesis entitled, **"Synthesis and Characterization of Bi doped $BaTiO_3$"** submitted by Mr. Dhiraj Kumar Rana in partial fulfillments for the requirements for the award of Master of Science Degree in Physics Department at National Institute of Technology, Rourkela is an authentic work carried out by him under my supervision and guidance.

To the best of my knowledge, the matter embodied in the project has not been submitted to any other University/ Institute for the award of any Degree or Diploma.

Rourkela
Date:

Prof. S. Panigrahi
Dept. of Physics
National Institute of Technology
Rourkela-769008

ACKNOWLEDGEMENT

With deep regards and profound respect, I avail this opportunity to express my deep sense of gratitude and indebtedness to Prof. S. Panigrahi, Department of Physics, National Institute of Technology Rourkela, for introducing the present project topic and for his inspiring guidance, constructive criticism and valuable suggestion throughout the project work. I most gratefully acknowledge his constant encouragement and help in different ways to complete this project successfully. I would like to acknowledge my deep sense of gratitude to Prof. Biplab Ganguly, Head, Department of Physics, National Institute of Technology Rourkela, for his valuable advices and constant encouragement for allowing me to use the facilities in the laboratory. I wish to thank all the faculty members & staffs of Department of Physics for their support and help during the project. It give me great pleasure to express my heartfelt gratitude to the laboratory mate , Mr. Tanmaya Badapanda and Mr. Senthil.V who have made it so easy to work in the laboratory by providing me with an utmost friendly humorous and amicable atmosphere to work in. Last but not the least; I would like to express my gratefulness to my parents for their endless support, without which I could not complete my project work. I would also like to thanks to my friends and all the Ph.D students in our physics department for their valuable help.

Rourkela Dhiraj Kumar Rana

Date:

CONTENTS

Abstract

$Ba_{1-x}Bi_{2x/3}TiO_3$ ceramics were prepared by solid state reaction route in different value of *x* (i.e., x = 0, 0.01, 0.025, 0.05, 0.075, 0.1). Structural property of all compositions is studied by XRD and surface morphology of the sintered pellets is studied by SEM analysis. XRD patterns reports the single phase tetragonal crystal system of the space group P4mm and pattern matched with the standard pattern JCPDS no. 05-0262 and it reveals the crystalline sizes decreases with increase the Bi concentration. SEM image shows the grain size decreases for x=0.01 and x=0.025 and increases with further addition of Bi concentration. The chemical composition of sintered pellets is analyzed by EDX. The temperature dependency dielectric study of $Ba_{1-x}Bi_{2x/3}TiO_3$ (i.e., x = 0, 0.025, 0.05) composition is studied. Dielectric constant and transition temperature decreases for x=0.025 and again increases for x=0.05. Curie constant values are calculated from the Curie Weiss law.

List of figure

List of table

CHAPTER-1

INTRODUCTION

Ferroelectricity was discovered in 1920 by J. Valasek. The first known ferroelectric material was Rochelle salt ($NaKC_4H_4O_6.4H_2O$). Unfortunately, Rochelle salt loses its ferroelectric properties if the composition is slightly changed, which made it rather unattractive for industrial applications. After that Barium titanate ($BaTiO_3$) was discovered to be ferroelectric behavior in 1945 by A Von Hippel and is perhaps the most commonly though of material when one thinks of ferroelectricity. $BaTiO_3$ is stable perovskite type, which is one of the fundamental crystal lattice structures. Perovskites form is the most important class of ferroelectric materials. The perfect perovskites structure follows the formula ABO_3' where A is a mono- or divalent and B is a tetra- or pentavalent metal. In (Fig.1) the A atoms form the corners of the cubic cells, B atoms are in the center and the oxygen atoms are situated in the faces centers of the cubic cell and the lattice is centre of symmetry so here no ferroelectricity can be observed.

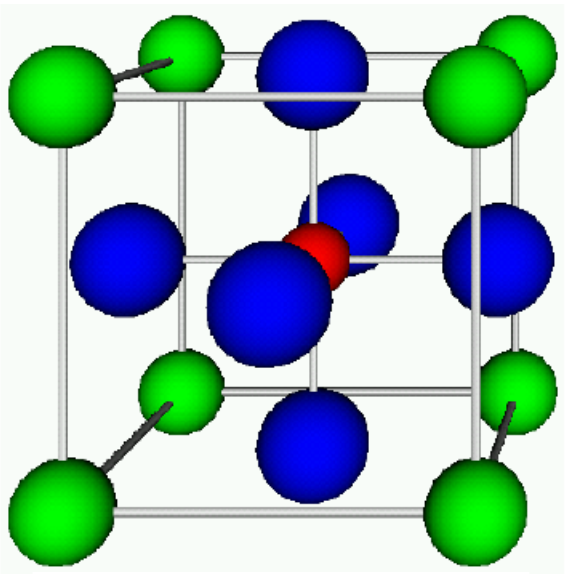

(Fig.1 Lattice structure of a symmetric perovskite crystal**)**

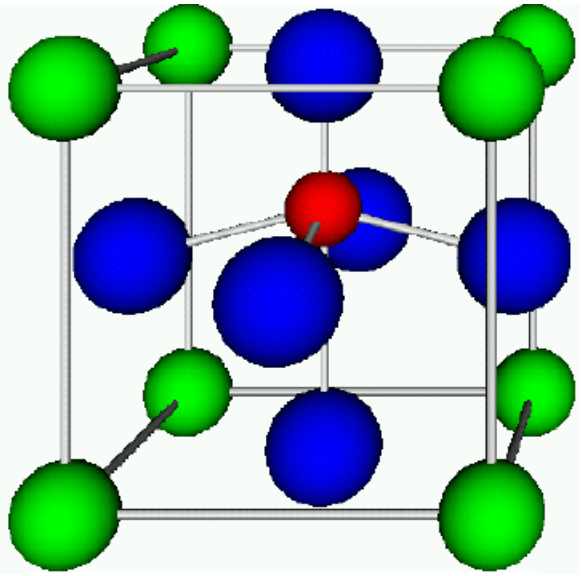

(Fig.2 Polarization of a tetragonal distorted crystal**)**

While In (Fig.2) shows that B atom is displace from its centre when the electric field is applied and the lattice is polarized. The phase is transform from cubic to tetragonal and the lattice is non-centre symmetry so here ferroelectricity should be observed.

While there are some 250+ materials that exhibit ferroelectric properties, some of the more common/significant materials include: Lead titanate($PbTiO_3$), Lead zirconate titanate (PZT), Lead lanthanum zirconate titanate (PLZT). Ferroelectricity has also been called Seignette electricity, as Seignette or Rochelle Salt (RS) was the first material found to show ferroelectric properties such as a spontaneous polarization on cooling below the Curie point, ferroelectric domains and a ferroelectric hysteresis loop.

The discovery of new classes of ferroelectrics advances in first principles theoretical techniques, and an expanded range of applications, mixed relaxor and ferroelectric ABO_3-type single crystals. A major breakthrough in the field of ferroelectricity occurred around 1960 with the publication of Cochran's seminal work. He advanced the concept that certain ferroelectric transitions are driven by instability of the crystal lattice against a soft optical phonon mode. These experimental techniques proved for the first time the microscopic nature of the static and dynamic properties of ferroelectric transitions. In spite of the fact that the soft mode concept was very successful in elucidating the microscopic mechanism not only for ferroelectric transitions but for structural phase transitions in general, the atomic-level origin of ferroelectricity, particularly in the ABO_3 perovskite, remained unclear. Most perplexing was the vastly different behaviors of seemingly very similar compounds such as $KtaO_3$ and $KNbO_3$, and $BaTiO_3$ and $SrTiO_3$. The domain of first-principles theory and the remarkable progress in the application of this theory to ferroelectrics in the past decade has paid significant dividends. Calculations for several ABO_3 compounds have identified hybridization between the oxygen 2p and transition-metal d states as the origin of the ferroelectric instability. Relaxor behavior generally results from crystalline disorder.

The occurrence of ferroelectricity is determined by a delicate balance between competing long-range Coulomb forces, which favor the ferroelectric state, and short-range repulsive forces, which favor the non-polar state. Hydrostatic pressure has been shown to be an excellent variable for tuning this balance and thereby providing new

insights into the underlying for tuning this balance and thereby providing new insights into the underlying physics. Additionally, there is intimate coupling between the polarization and lattice strain (or volume).

Ferroelectric materials may be divided into two classes: classical ferroelectrics and relaxors

i. Typically relaxors have at least one crystallographic site that is occupied by two or more ions. In addition to usual application for classical ferroelectrics, relaxors have great interest for dielectrics in capacitors and actuators

ii. Most relaxors lead based ceramics such as $PbMg_1/3Nb_{2/3}O_3$ (PMN) and derived compounds. Or Pb $(M`_1/2M"_{1/2})O_3$ with long range polar order. However, these compositions have the obvious disadvantages associated with the volatility and toxicity of PbO. Therefore, much current research is directed towards more environmentally friendly Pb-free relaxor materials.

1.1 Ferroelectric

Most materials are polarized linearly with external electric field; nonlinearities are insignificant. This is called dielectric polarization (Fig.3). Some materials, known as paraelectric materials, demonstrate a more pronounced nonlinear polarization. The electric permittivity, corresponding to the slope of the polarization curve, is thereby a function of the external electric field. In addition to being nonlinear, ferroelectric materials demonstrate a spontaneous (zero field) polarization. Such materials are generally called pyroelectrics. The distinguishing feature of ferroelectrics is that the direction of the spontaneous polarization can be reversed by an applied electric field, yielding a hysteresis loop. Typically, materials demonstrate ferroelectricity only below a certain phase transition temperature, called the Curie temperature, T_c, and are paraelectric above this temperature.

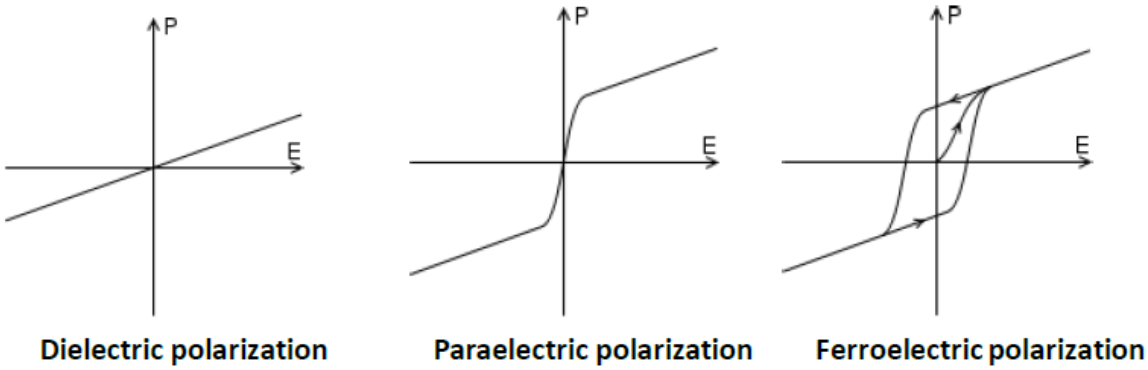

(Fig.3 Polarization Vs Electric field (P-E) loop for different materials**)**

***Ferroelectric Crystal*:** *A ferroelectric crystals is crystals that possess reversible spontaneous polarization as exhibited by a dielectric hysteresis loop* (reversibility of the polarization).

Ferroelectric crystals possess regions with uniform polarization called ferroelectric domains. Within a domain, all the electric dipoles are aligned in the same direction. There may be many domains in a crystal separated by interfaces called domain walls. A ferroelectric single crystal, when grown, has multiple ferroelectric domains. A single domain can be obtained by domain wall motion made possible by the application of an appropriate electric field. A very strong field could lead to the reversal of the polarization in the domain, known as domain switching. All ferroelectric materials are pyroelectric, however, not all pyroelectric materials are ferroelectric. Below a transition temperature called the Curie temperature ferroelectric and pyroelectric materials are polar and possess a spontaneous polarization or electric dipole moment. The non-polar phase encountered above the Curie temperature is known as the paraelectric phase. The direction of the spontaneous polarization conforms to the crystal symmetry of the material, while the reorientation of the spontaneous polarization is a result of atomic displacements. The magnitude of the spontaneous polarization is greatest at temperatures well below the Curie temperature and approaches zero as the Curie temperature is neared.

The most characteristics property of a ferroelectric is the hysteresis loop is shown in (fig. 4). As the electric field strength is increased, the domains start to align in the positive direction giving rise to a rapid increase in the polarization. At very high field levels, the polarization reaches a saturation value (P_s). The polarization does not fall to

zero when the external field is removed. At zero external field, some of the domains remain aligned in the positive direction, hence the crystal will show a remnant polarization P_r. The crystal cannot be completely depolarized until a field of magnitude is applied in the negative direction. The external field needed to reduce the polarization to zero is called the coercive field strength Ec. If the field is increased to a more negative value, the direction of polarization flips and hence a hysteresis loop is obtained. The value of the spontaneous polarization $\mathbf{P_s}$ is obtained by extrapolating the curve onto the polarization axes.

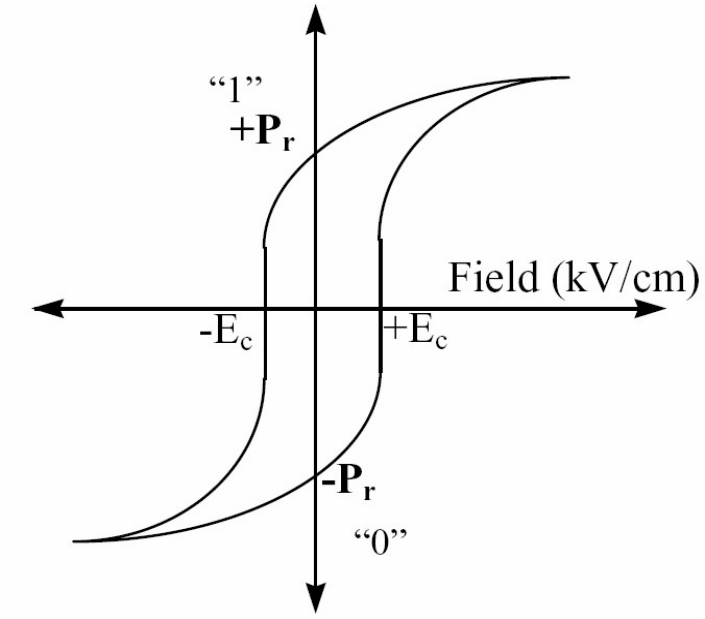

(Fig.4 Polarization vs. Electric Field (P-E) hysteresis loop for a typical ferroelectric crystal**)**

The relationship between D (or P) and E is linear up to relatively large fields. However, in the case of ferroelectrics ε and χ must be defined more precisely owing to the more complicated relationship between D (or P) and E. For most purposes of this review, ε and c are defined as the slopes of the D vs. E and P vs. E curves, respectively, at the origin, i.e., the initial values.

$$\varepsilon = (\partial d/\partial E)_{E=0} \text{ and } \chi = (\partial P/\partial E)_{E=0} \text{ ---------- (1.1)}$$

They are determined from measurements made at very low ac fields so as not to reverse any domains. Although ferroelectric crystals are a widely varied group, they posses a number a general characteristics properties, among these are the following:

- The hysteresis loop disappears at a certain temperature, the Curie point T_c, above which the crystal behaves as a normal dielectric. It should be noted, however, that in some crystals melting or chemical decomposition may occur before the Curie point is reached.
- At T_c a ferroelectric crystal transforms to a phase of higher symmetry. This higher temperature phase is usually nonpolar, or paraelectric (PE).
- The polar crystal structure of a ferroelectric can be derived from the high-temperature PE structure by a slight distortion of the crystal lattice. This is the main reason behind the success of the phenomenological theory of ferroelectricity which assumes that the same free energy function is applicable for both the FE and PE phases.
- Ferroelectrics generally have a large ε (or χ), which rises to a peak value at T_c.
- Above T_c, ε of a ferroelectric (measured along the polar axis) usually obeys the Curie-Weiss law $\varepsilon = C/(T-T_0)$, where C and T_0 are the Curie-Weiss constant and Curie-Weiss temperature, respectively.

Finally, we should mention that there are substances which, on cooling, undergo a transition from a nonpolar to an antipolar state. In this state the crystal has a superlattice consisting arrays of antiparallel dipoles. If, in a given crystal, the coupling energy between these arrays is comparable to that of the polar case, then the crystal is said to be antiferroelectric (AFE). An antiferroelectric crystal can usually be made ferroelectric by the application of a sufficiently large electric field.

1.2 Crystal Symmetry

The lattice structure described by the Bravais unit cell of the crystal governs the crystal symmetry.

Solid matter can be described as:

a. **Amorphous:** The atoms are arranged in a random way similar to the disorder we find in a liquid. Glasses are amorphous materials.
b. **Crystalline:** The atoms are arranged in a regular pattern, and there is as smallest volume element that by repetition in three dimensions describes the crystal. e.g. we can describe a brick wall by the shape and orientation of a single brick. This smallest volume element is called a unit cell. The dimensions of the unit cell is described by three axes : a, b, c and the angles between them α, β, γ.

There are thirty-two point groups (Fig. 5) can be classified into (a) crystals having a center of symmetry and (b) crystals which do not possess a center of symmetry. Crystals with a center of symmetry include the 11 point groups labeled centrosymmetric. These point groups do not show polarity. The remaining 21 point groups do not have a center of symmetry (i.e. non-centrosymmetric). A crystal having no center of symmetry possesses one or more crystallographically unique directional axes. Out of these, 20 classes are piezoelectric (the one exception being cubic class 432). Piezoelectric crystals have the property that the application of mechanical stress induces polarization, and conversely, the application of an electric field produces mechanical deformation. Of the 20 piezoelectric classes, 10 have a unique polar axis, such crystals are called polar crystals as they show spontaneous polarization, i.e. polarized in the absence of an electric field. Crystals belonging to these 10 classes are called pyroelectric.

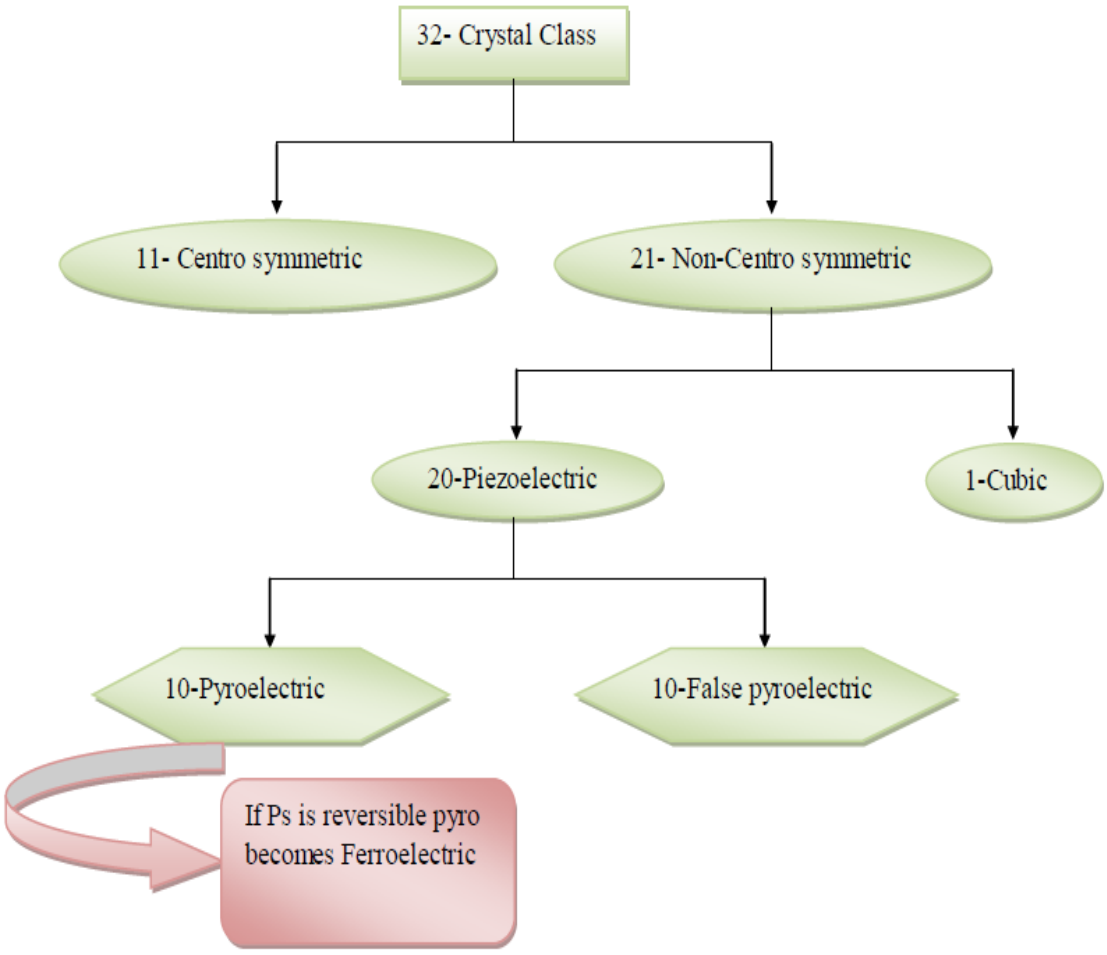

(Fig.5 Crystal point group**)**

The intrinsic polarization of pyroelectric crystals is often difficult to detect experimentally because of the neutralization of the charges on the crystal surfaces by free charges from the atmosphere and by conduction within the crystal. However, because the polarization is a function of temperature, it is often possible to observe the spontaneous moment in these crystals by changing the temperature, hence the name pyroelectric. Ferroelectric crystals belong to the pyroelectric family, but they also exhibit the additional property that the direction of the spontaneous polarization can be reversed by the application of an electric field.

1.3 Relaxor Ferroelectrics

High and broad maxima in temperature dependence of both components of complex permittivity $\varepsilon^* = \varepsilon' - i\varepsilon''$ and their shift to higher temperatures with raising measuring frequency is a typical feature of relaxor ferroelectrics (RFEs). Relaxor ferroelectric exhibit many properties similar to those of spin and dipolar glasses. Relaxor behavior is normally FE materials results from compositionally induced disorder or frustration. This behavior has been observed and studied mist extensively in disordered ABO_3 perovskite ferroelectrics and is also seen in mixed crystals of hydrogen-bonded FEs and AFEs, the so-called phonic glasses. In this section we restrict our comments largely to the ABO_3 oxides. Most of the RFEs with potential piezoelectric applications are lead-based compounds with the perovskite structure; however there is currently an increased need for more environmental friendly lead-free compounds.

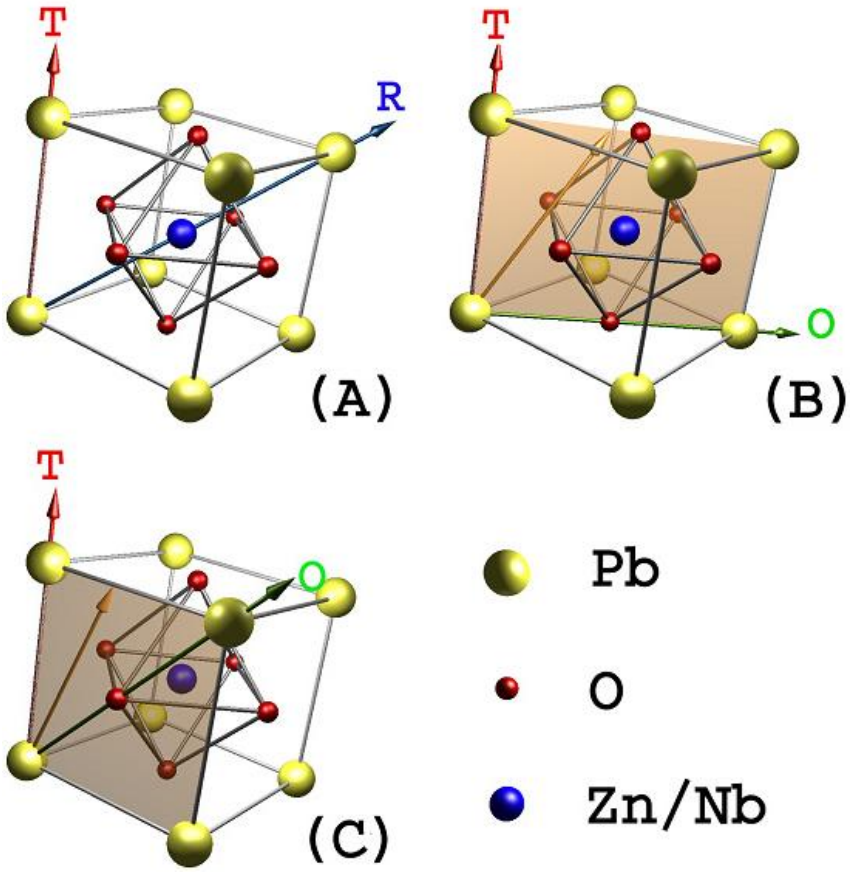

(Fig.6 Different polarization directions {marked by arrows} in the relaxor perovskite structure**)**

In the ABO_3 oxides (Fig.6), shows the different polarization directions (marked by arrows) in the relaxor perovskite structure. (A) Polarizations along T and R direction (B) The MA phase, for which the polarization lies in the (110) plane, can be obtained by combining T and O direction (C) The MC phase, for which the polarization lies in the (100) plane, can also be obtained by combining T and O direction. Due to polarizabilities at both the A and B lattice sites produces dipolar defects and can introduce a sufficiently high degree of disorder so as to break translational symmetry and prevent the formation of a long-range ordered state. Instead, the dipolar motion in such systems freezes into a glass-like state on cooling below the transition temperature, T_m.

In these highly polarizable host lattices, the presence of a dipolar impurity on a given site can induce dipoles in a number of adjacent unit cells within a correlation length of that site. We accept the dipolar motion within this correlation length to be correlated, leading to the formation of polar nanodomains. Indeed, such nanodomains have been observed in many ABO_3 relaxors at temperatures far above the peak in $\varepsilon'(T)$, and their occurrence is now considered to be crucial to the understanding of the properties of relaxors. We picture a distribution of sizes of such nanodomains in which the orientational degrees of freedom are correlated within each domain, but uncorrelated across the various domains. At sufficiently low temperatures, the dipolar motion within each domain freezes, resulting in the formation of an orientational glass (relaxor) state. Such a state is characterized by a distribution of relaxation times related to the sizes of the nanodomains. Two important characteristics of this relaxor state that distinguish it from simple dipolar glasses or spin glasses are the predominant existence of the dipolar nanodomains (vs. largely individual dipoles or spins) and the presence of some degree of cooperative freezing of the orientational degrees of freedom. Evidence of this cooperative effect comes from the observation of some remnant polarization in electric field hysteresis loops. It should be noted, however, that such evidence is also seen in systems of random dipoles in low polarizability hosts for doped alkali halides with sufficiently high concentration of dipoles.

In order to be a good piezoelectric material, the lattice shape must be able to change significantly in response to an external electric field. Theoretical work has suggested that phase instability may be responsible for this effect. The directional

dependence of sound wave propagation in the current study provides strong evidence that such phase instability does exist and is indeed induced by the polar nano regions.

Table 1 Difference between normal and relaxor ferroelectric

Property	**Normal Ferroelectric**	**Relaxor Ferroelectric**
Dielectric temperature dependence	Sharp 1^{st} or 2^{nd} order transition at Curie point T_c	Broad diffused phase transition at Curie maxima
Dielectric frequency dependence	Weak Frequency dependence	Strong frequency dependence
Dielectric Behavior in paraelectric range ($T > T_c$)	Follows Curie - Weiss law	Follows Curie - Weiss square law
Remnant polarization (P_r)	Strong P_r	Weak P_r
Scattering of light	Strong anisotropy	Very weak anisotropy to light
Diffraction of X-Rays	Line splitting due to deformation from paraelectric to ferroelectric phase	No X-Ray line splitting

This intrinsic instability apparently helps to facilitate the field-induced structural change and contributes to the large piezoelectric response. In table-1 shows the properties of relaxors are contrast to some of their properties with those of normal ferroelectrics.

The contrast is as follows:

- The P-E hysteresis loop (Fig.4) is the signature of a ferroelectric in the low-temperature Fe phase. The large remnant polarization, P_r, is a manifestation of the cooperative nature of the FE phenomenon. A relaxor, on the other hand, exhibits a so-called slim-loop. For sufficiently high electric fields the nanodomains of the relaxor can be oriented with the field leading to large polarization; however, on removing the field most of these domains reacquire their random orientations resulting in a small P_r. The small P_r is evidence for the presence of some degree of cooperative freezing of dipolar (or nanodomain) orientations.
- The saturation and remnant polarizations of a ferroelectric decrease with increasing temperature and vanish at the FE transition temperature (T_c). The vanishing of P at T_c is continuous for a second-order phase transition and discontinuous for a first-order transition. No polar domains exist above T_c. By contrast, the field-induced polarization of a relaxor decreases smoothly through the dynamic transition temperature T_m and retains finite values to rather high temperatures due to the fact that nano-size domains persist to well above T_m.

1.4 Barium Titanate:

Barium titanate (BT) is one of the most studied ferroelectric materials which have been used in various forms, e.g. bulk, thin and thick films, powder, in a number of applications. Since the discovery of high dielectric property of $BaTiO_3$ ceramic, many investigators have tried to modify this compound by different means, in order to achieve stable capacitors with satisfactory operational capacity and Barium titanate (BT) has become one of the most important electroceramics since the discovery of its versatility in multilayer ceramic capacitors (MLCC), positive temperature coefficient of resistance (PTCR) thermistors, piezoelectric sensors, transducers, actuators and ferroelectric random access memories (FRAM) and electro-optic devices. Its properties can be further improved by doping or by controlling its microstructural characteristics by varying process parameters. A huge increase in the research on ferroelectric materials came in the 1950's, leading to the common use of Barium Titanate ($BaTiO_3$) based ceramics in capacitor applications and piezoelectric transducer devices.

Barium titanate has the appearance of a white powder or transparent crystals. It is insoluble in water and soluble in concentrated sulfuric acid.

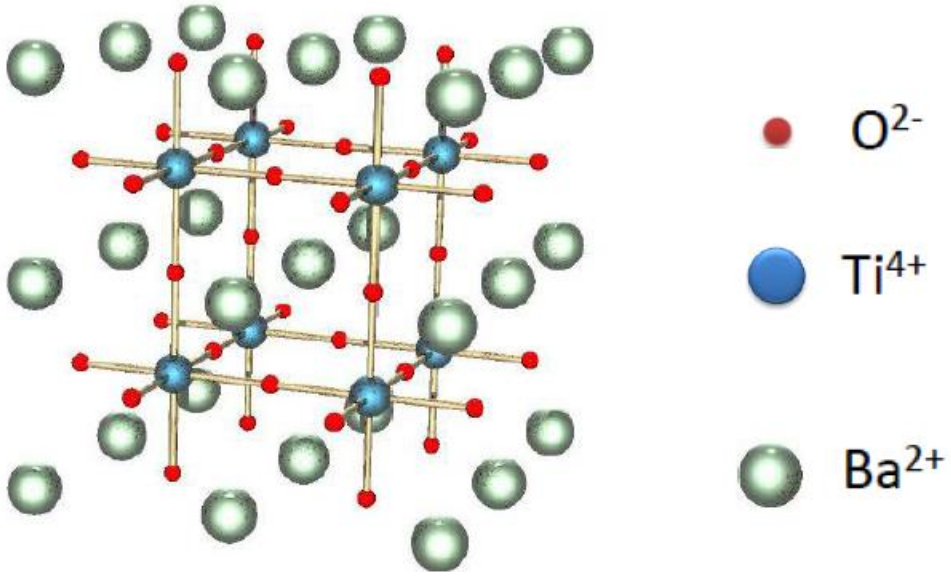

(Fig.7 Structure of $BaTiO_3$ **)**

Barium Titanate is an oxide of barium and titanium with the chemical formula $BaTiO_3$ as shown in Fig. 7. It is a ferroelectric ceramic material, with a photorefractive effect and piezoelectric properties. It has five phases as a solid, listing from high temperature to low temperature: hexagonal, cubic, tetragonal, orthorhombic, and rhombohedral crystal structure. All of the structures exhibit the ferroelectric effect except cubic. Barioperovskite is a very rare natural analogue of $BaTiO_3$, found as micro inclusions inbenitoite.

Barium titanate ($BaTiO_3$) has a paraelectric cubic phase above its Curie point of about 130° C. In the temperature range of 130° C to 0° C the ferroelectric tetragonal phase and between 0° C and -90° C, the ferroelectric orthorhombic phase is stable.

The spontaneous polarization on cooling BaTiO3 below the Curie point T_c is due to changes in the crystal structure. As shown in (Fig.8) the paraelectric cubic phase is stable above 130° C with the center of positive charges (Ba^{2+} and Ti^{4+} ions) coinciding with the center of negative charge (O^{2-}). On cooling below the Curie point T_c, a tetragonal structure develops where the center of $Ba^{2+}$and Ti^{4+} ions are displaced relative to the O^{2-} ions, leading to the formation of electric dipoles. Spontaneous polarization

developed is the net dipole moment produced per unit volume for the dipoles pointing in a given direction.

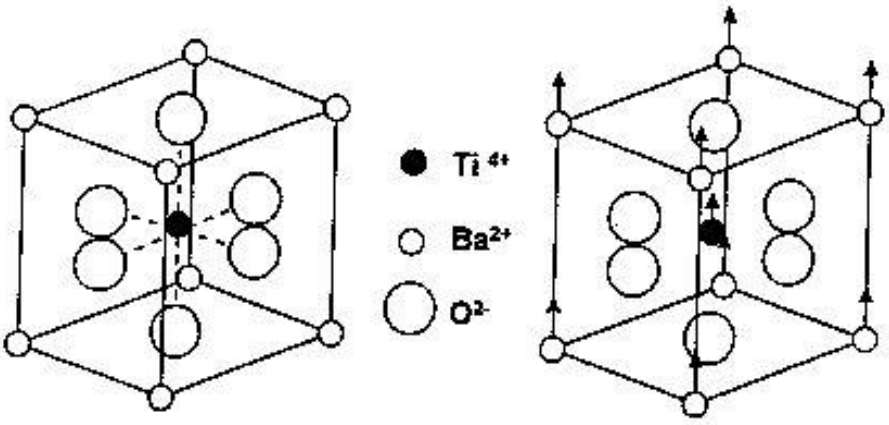

(a) (b)

(Fig.8 The crystal structure of BaTiO3 (a) above the Curie point (b) below the Curie point**)**

Barium Titanate is used as a dielectric material for ceramic capacitors, and as a piezoelectric material for microphones and other transducers. The Curie point of Barium Titanate is 130 °C. As a piezoelectric material, it was largely replaced by lead zirconate titanate, also known as PZT. Polycrystalline Barium Titanate displays positive temperature coefficient, making it a useful material for thermistors and self-regulating electric heating systems. Fully-dense nanocrystalline Barium Titanate has 40% higher permittivity than the same material prepared in classic ways. Barium Titanate crystals find use in nonlinear optics. The material has high beam-coupling gain, and can be operated at visible and near-infrared wavelengths. It has the highest reflectivity of the materials used for self-pumped phase conjugation (SPPC) applications. It can be used for continuous-wave four-wave mixing with milliwatt-range optical power. For photorefractive applications, Barium Titanate can be doped by various other elements, e.g. iron.

CHAPTER-2

THESIS OBJECTIVE

- ✓ To synthesis the high dielectric constant material ($BaTiO_3$) by solid state reaction route.
- ✓ To characterize the synthesized materials like XRD for phase formation, SEM for surface morphology, EDX for chemical analysis and Electrical study for dielectric constant and transition temperature.

CHAPTER-3

EXPERIMENTAL TECHNIQUE

A basic introduction about the experiment use in synthesized and characterized the $Ba_{1-x}Bi_{2x/3}TiO_3$ ceramic compound.

3.1 Synthesis methods:

3.1.1 Ball Mill

A ball mill is a type of grinder used to grind materials into extremely fine powder for use in mineral dressing processes, paints, pyrotechnics, and ceramics. Ball mills rotate around 300 rpm at horizontal axis, partially filled with the material to be ground plus the grinding medium. Different materials are used as media, including ceramic balls, flint pebbles and stainless steel balls. An internal cascading effect reduces the material to a fine powder. The difference in speeds between the balls and grinding jars produces an interaction between frictional and impact forces, which releases high dynamic energies. The interplay between these forces produces the high and very effective degree of size reduction of the planetary ball mill.

3.1.2 Calcination

Calcination is the process in which a material is heated to a temperature below its melting point to effect the thermal decomposition or the phase transition other than melting point, or removal of a volatile fraction. Calcination is to be distinguished from roasting, in which more complex gas-solid reactions take place between the furnace atmosphere and the solids. Calcination reactions usually take place at or above the thermal decomposition temperature or the transition temperature (for phase transitions). This temperature is usually defined as the temperature at which the standard Gibbs free energy for a particular calcination reaction is equal to zero.

3.1.3 Sintering

When thermal energy is apply to powder compact, the compact is densified and the average grain size is increases, this process is called sintering and the basic phenomena occurring form this process is densification and grain growth. This is process used to produced density control materials or compound from metal or ceramic powder by applying thermal energy. Sintering aims to produce sintered part with reproducible and if possible designed a microstructure through control the sintering variables.

Microstructural control means control of gain size, sintered density, and size and distribution of other phases including pores. In most of the cases microstructural control prepare a full dense body with fine grain structure.

Table 2 For Variables affecting in sintering and microstructure

<table>
<tr><td colspan="2">Sintering process</td></tr>
<tr><td rowspan="2">Variables related to raw materials
(materials variables)</td><td>Powder:
Shape, size, size distribution, agglomeration, mixedness, etc.</td></tr>
<tr><td>Chemistry:
Composition, impurity, non-stoichiometry, homogeneity, etc.</td></tr>
<tr><td>Variables related to sintering condition
(process variables)</td><td>Thermodynamic:
Temperature, time, pressure, atmosphere, heating and cooling rate, etc.</td></tr>
</table>

3.2 Characterization methods:

The structure provides a variety of concepts, which describes on various scales; its mechanical, chemical or electrical may depends strongly on its internal structure. An understanding of the structure of the material has become essential in the worked of novel materials. A wide range of experimental methods are available for the evaluation of structure of material with high accuracy and precision. The structure and morphology studies are preformed by using various techniques such as X-ray diffraction analysis (XRD) and scanning electron microscopy (SEM). The analysis of the elemental composition present in the sample is often aided through the use of the diffraction technique with energy dispersive analysis (EDX). The electrical measurement can be done through HIOKI LCR meter in different temperatures.

3.2.1 XRD Analysis

X-ray diffraction methods are especially significant for the analysis of solid materials in the forensic science. Small sample quantities or tiny sample areas can be successfully analyzed as well as large quantities of materials. When X-rays interact with a crystalline substance (Phase), one gets a diffraction pattern.

The angle between the beam axis and the ring is called the *scattering angle* and in X-ray crystallography always denoted as 2θ. In accordance with Bragg's law when X-rays hit an atom, they make the electronic cloud move as does any electromagnetic wave. The interference is constructive when the phase shift is a multiple of 2π; this condition can be expressed by Bragg's law:

$$n\lambda = 2d \sin\theta$$

Where n is an integer determined by the order given, λ is the wavelength of the X-rays d is the spacing between the planes in the atomic lattice, and θ is the angle between the incident ray and the scattering planes.

An electron in an alternating electromagnetic field will oscillate with the same frequency as the field. When an X-ray beam hits an atom, the electrons around the atom start to oscillate with the same frequency as the incoming beam. In almost all directions we will have destructive interference, that is, the combining waves are out of phase and there is no resultant energy leaving the solid sample. However the atoms in a crystal are arranged in a regular pattern, and in a very few directions we will have constructive interference. The waves will be in phase and there will be well defined X-ray beams leaving the sample at various directions. Hence, a diffracted beam may be described as a beam composed of a large number of scattered rays mutually reinforcing one another. The orientation and interplanar spacing of these planes are defined by the three integers (h k l) called indices. A given set of planes with indices (h k l) cut the a-axis of the unit cell in h sections, the b-axis in k sections and the c-axis in l sections. A zero indicates that the planes are parallel to the corresponding axis. e.g. the (2 2 0) planes cut the a– and the b– axes in half, but are parallel to the c– axis.

There are many factors that determine the width B of a diffraction peak. These include:

- Instrumental factors
- The presence of defects to the perfect lattice
- Differences in strain in different grains
- The size of the crystallites

It is often possible to separate the effects of size and strain. Where size broadening is independent of q (K=1/d), strain broadening increases with increasing q-values. In most cases there will be both size and strain broadening. It is possible to separate these by combining the two equations in what is known as the Hall-Williamson method:

$$B.\cos\theta = \frac{k\lambda}{L} + \eta\,.\sin\theta$$

Thus, when we plot B . cos(θ) vs sin(θ) we get a straight line with slope η and intercept $\frac{k\lambda}{L}$.

The expression is a combination of the Scherrer Equation for size broadening and the Stokes and Wilson expression for strain broadening. The value of η is the lattice strain and the value of L represents the size of the crystalline. The value of constant k is taken as 0.9.

3.2.2 Scanning Electron Microscope (SEM)

The scanning electron microscope (SEM) is a type of electron microscope that images the sample surface by scanning it with a high-energy beam of electrons in a raster scan pattern. The electrons interact with the atoms that make up the sample producing signals that contain information about the sample's surface topography, composition and other properties such as electrical conductivity. The types of signals produced by an SEM include secondary electrons, back-scattered electrons (BSE), characteristic X-rays, light (cathodoluminescence), specimen current and transmitted electrons.

The SEM has a large depth of field, which allows a large amount of the sample to be in focus at one time. The SEM also produces images of high resolution, which means that closely spaced features can be examined at a high magnification. Preparation of the samples is relatively easy since most SEMs only require the sample to be conductive. The

combination of higher magnification, larger depth of focus, greater resolution, and ease of sample observation makes the SEM one of the most heavily used instruments in research areas today.

3.2.3 Energy Dispersive X-ray Spectroscopy (EDS or EDX)

EDS or EDX is an analytical technique used for the elemental analysis or chemical characterization of a sample. It is one of the variants of X-ray fluorescence spectroscopy which relies on the investigation of a sample through interactions between electromagnetic radiation and matter, analyzing X-rays emitted by the matter in response to being hit with charged particles. Its characterization capabilities are due in large part to the fundamental principle that each element has a unique atomic structure allowing X-rays that are characteristic of an element's atomic structure to be identified uniquely from one another.

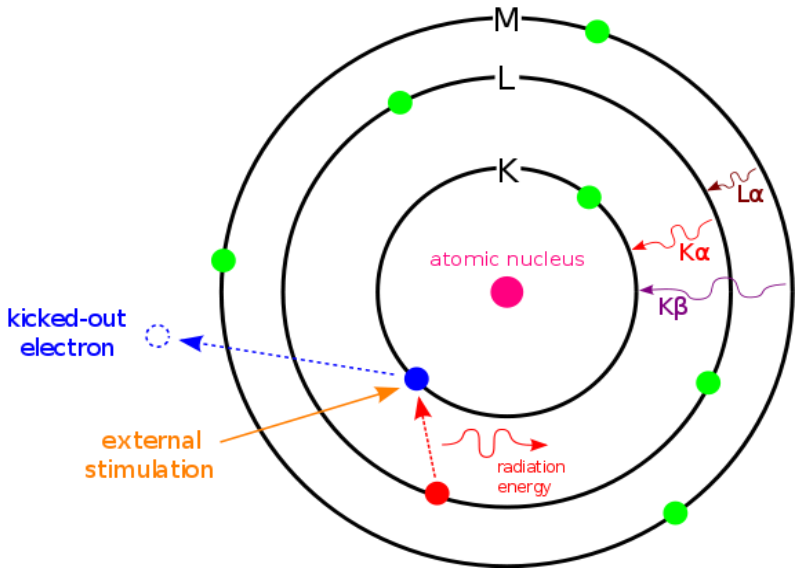

(Fig.9 Principle of EDS**)**

The incident beam may excite an electron in an inner shell, ejecting it from the shell while creating an electron hole. An electron from an outer, higher-energy shell then fills the hole, and the difference in energy between the higher-energy shell and the lower energy shell may be released in the form of an X-ray. The number and energy of the X-rays emitted from a specimen can be measured by an energy dispersive spectrometer. As the energy of the X-rays are characteristic of the difference in energy between the two

shells, and of the atomic structure of the element from which they were emitted, this allows the elemental composition of the specimen to be measured.

3.2.4 Dielectric

A dielectric is an electrical insulator that may be polarized by the action of an applied electric field. When a dielectric material is placed in an electric field, electric charge do not flow through the material, as in a conductor, but only slightly shift from their average equilibrium positions causing dielectric polarization: positive charges are displaced along the field and negative charges shift in the opposite direction.

The study of dielectric properties is concerned with the storage and dissipation of electric and magnetic energy in materials. It is important to explain various phenomena in electronics, optics, and solid-state physics. A dielectric material is a substance that is a poor conductor of electricity, but an efficient supporter of electrostatic fields. If the flow of current between opposite electric charge poles is kept to a minimum while the electrostatic lines of flux are not impeded or interrupted, an electrostatic field can store energy. This property is useful in capacitors, especially at radio frequencies. Dielectric materials are also used in the construction of radio-frequency transmission lines.

3.3 Experimental work

The Bi doped $BaTiO_3$ ceramic were prepare by solid state reaction method by taking three raw materials such as (i) Barium Carbonate ($BaCO_3$), (ii) Titanium dioxide (TiO_2) and (iii) Bismuth Oxide (Bi_2O_3). For the combination of these three raw materials $Ba_{1-x}Bi_{2x/3}TiO_3$ ceramic compound were formed, where 'x' is the Bi concentration in $BaTiO_3$ ceramic compound (i.e, x = 0, 0.01, 0.025, 0.05, 0.075, 0.1). For synthesis of $Ba_{1-x}Bi_{2x/3}TiO_3$ ceramic compound first we used ball-mill for mixing and grinded the milled powder into extremely fine powder. The prepare powder were kept in programmable furnace for calcinations process and heated at temperature below melting point of the sample for the phase formation and removal of a volatile fraction. For making pellets used binder i.e, poly vinyl alcohol (PVA) solution mix with powder and to make pellets by using hydraulic pressure, to applying around 5 ton pressure for 3 minutes. To know the phase formation of prepare (calcinations) sample used XRD analysis technique. Use SEM for surface morphology and EDX for chemical composition

of $Ba_{1-x}Bi_{2x/3}TiO_3$ ceramic compound and at last measured the electrical properties i.e, dielectric and curie constant.

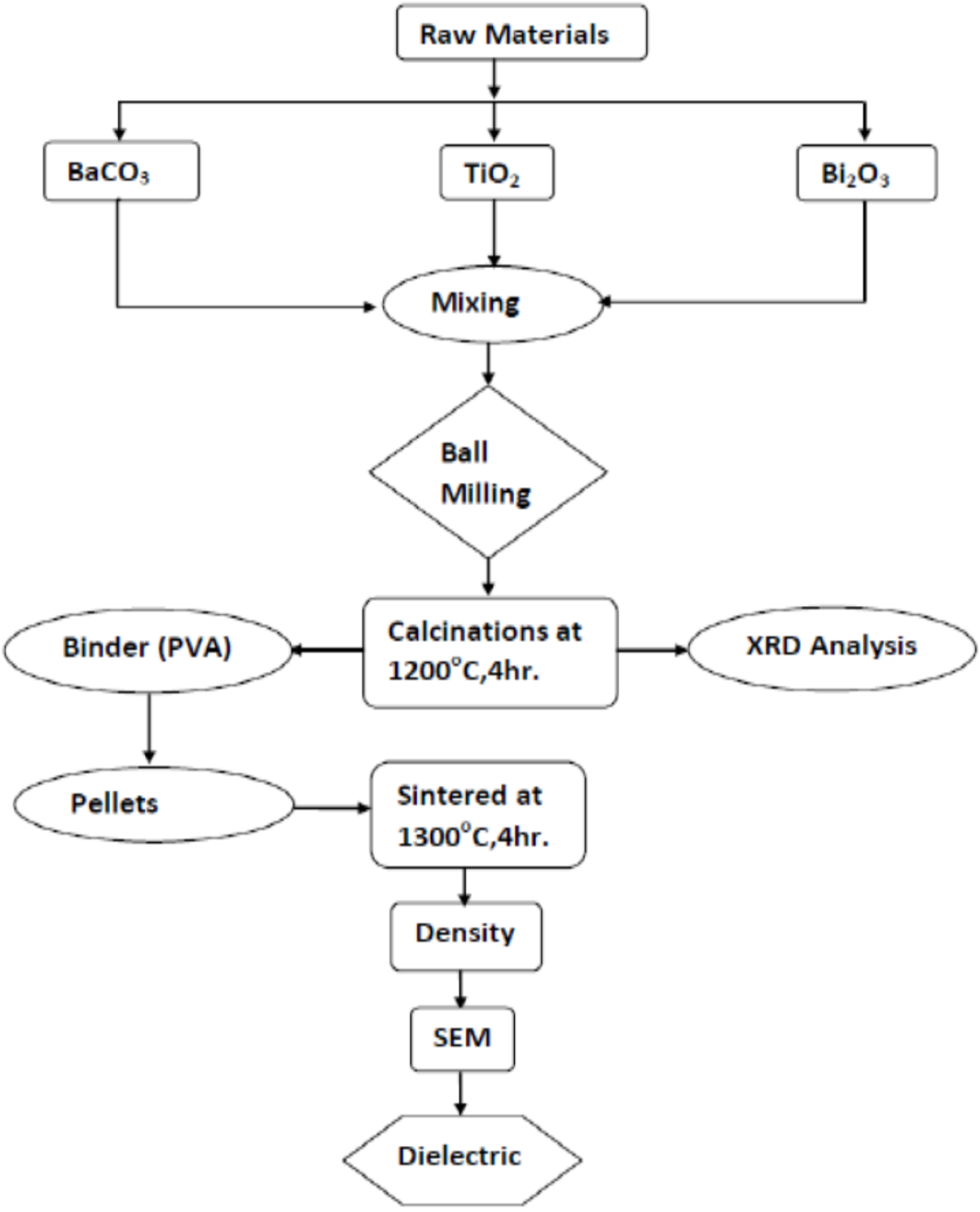

(Fig.10 Flowchart for the synthesis of Bi doped $BaTiO_3$ceramic**)**

CHAPTER-4
RESULTS AND DISCUSSION

4.1 XRD Analysis

The $Ba_{1-x}Bi_{2x/3}TiO_3$ ceramics were prepared by solid state reaction route. The synthesized powders were characterized by X-ray diffraction using a PANALYTIC diffractometer. XRD pattern were obtained using Cu Kα radiation and the Fig.11 show the XRD pattern of the Bi doped $BaTiO_3$ range from 20-80^o in 2θ scale at the rate of 0.04^o/second. According to JCPDS no.05-0626, all the peaks in the patterns are matching and its showing purely tetragonal single phase crystal related to tetragonal $BaTiO_3$. The crystal single phase crystals of the $Ba_{1-x}Bi_{2x/3}TiO_3$ ceramics are tetragonal symmetry in the space group P4mm. No evidence of the precursor phase $BaCO_3$, TiO_2 or Bi_2O_3 was detected by XRD and all the matched *hkl* values are indexed in the Fig.11. From Fig.12, it is well known that the tetragonal phase was identified by an analysis of the peaks [002] and [200] at the 2θ from 44.5-46^o. The splitting of [002] and [200] peaks indicates the tetragonal phases. While increasing the concentration of Bi in $BaTiO_3$, the intensity of is peak [002] at 44.9 is minimizing. This minimization indicates the conversion of tetragonal phase to cubic phase after the certain limit of doping concentration. Fig.13 and 14 shows the lattice parameter as well as the unit cell volume results of $Ba_{1-x}Bi_{2x/3}TiO_3$ ceramics. These data were estimated through the *CHEKCELL* program using the regression diagnostics combined with nonlinear least squares. The ratio of *c* and *a* gives the value of more than 1, it is showing the tetragonal phases and the volume of the tetragonal is strongly related to *a* and *c* parameters. Table 3, shows the parameters about the peak position, FWHM, a, b, c parameters, volume, c/a, crystallite size, lattice strain, D_{hkl} and d_{hkl} for all x values at the major peaks of the XRD patterns at 31.4^o. In Fig.15 variation of crystalline size as a result of Bi substitution is clearly seen. Crystalline size decreases with increasing concentration of the Bi in $BaTiO_3$ and these effects is clearly seen in the peak broadening of Fig.12.

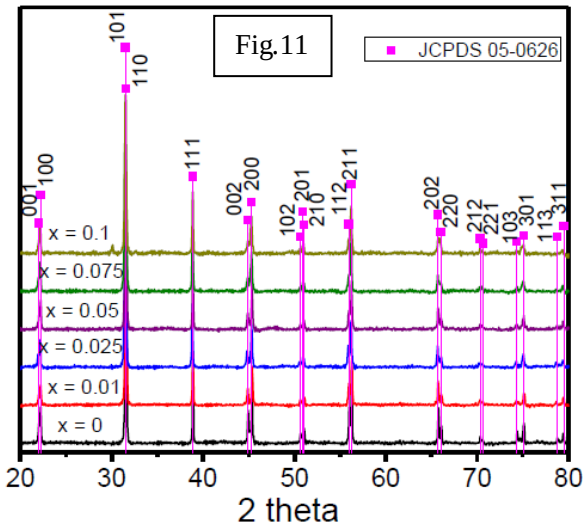

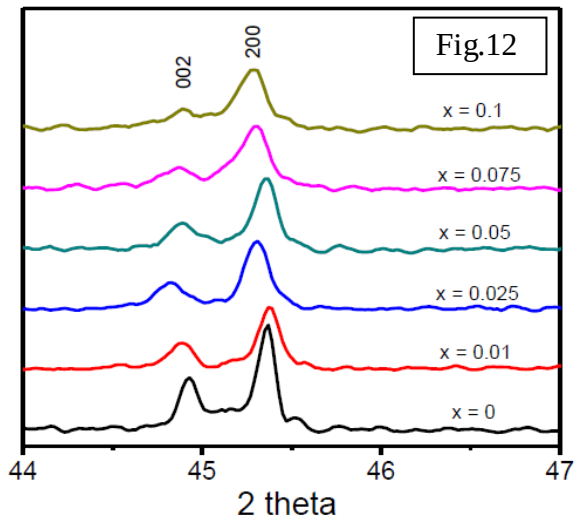

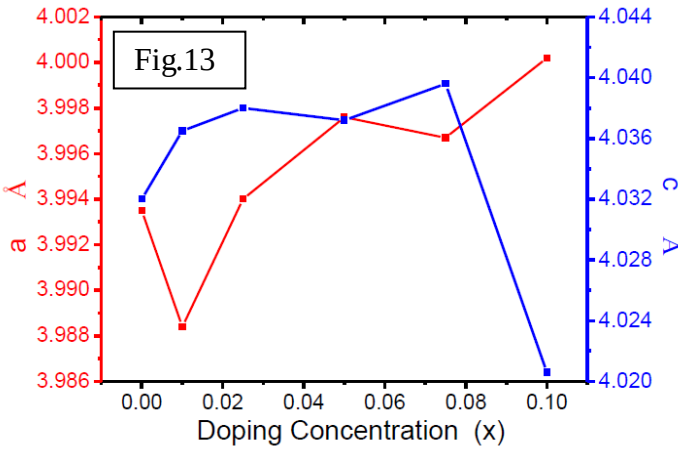

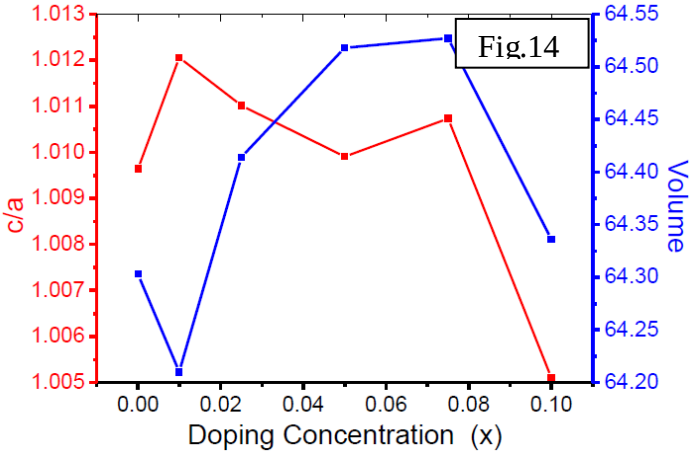

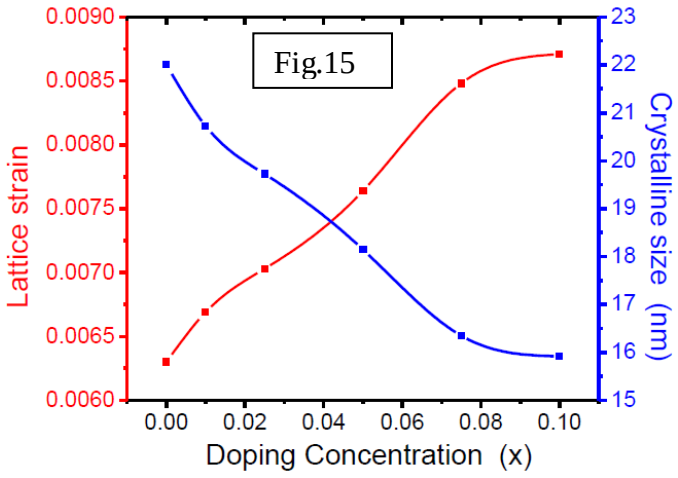

(Fig. 11,12 XRD pattern

Fig.13 Composition Vs a & c

Fig.14 Composition Vs c/a & volume

Fig.15 Composition Vs lattice strain & crystalline**)**

Table 3 Peak position, FWHM, a, b, c, volume, c/a, crystalline, lattice strain, d_{hkl} *and* D_{hkl} parameters for all composition of x

Sample	Conc. (x)	2θ in degree	FWHM	Θ in rad	a = b	c	volume	c/a	Crystalline (in m)	Lattice strain	d_{hkl}	D_{hkl}
i	0	31.5099	0.00209	0.274836	3.9947	4.0308	64.32201	1.009037	2.20E-08	0.0063	2.838357	689.2854
ii	0.01	31.4899	0.00251	0.274662	3.9924	4.0376	64.35635	1.011322	2.07E-08	0.00669	2.840114	573.9186
iii	0.025	31.4300	0.00251	0.274139	3.994	4.038	64.41432	1.011017	1.97E-08	0.00703	2.84539	573.8342
iv	0.05	31.4899	0.00293	0.274662	3.994	4.038	64.41432	1.011017	1.81E-08	0.00764	2.840114	491.6504
v	0.075	31.4699	0.00377	0.274487	3.9966	4.0395	64.52217	1.010734	1.64E-08	0.00848	2.841873	382.0862
vi	0.1	31.4915	0.00377	0.274676	4.0002	4.0214	64.34883	1.0053	1.59E-08	0.00871	2.839973	382.1065

4.2 SEM and EDX

Fig.16 shows the surface structures of all sintered pellets at 1300^{o}C for 4 hours. The microstructure of the sintered specimens of the $BaTiO_3$ with x=0 to 0.1, Bi were shown the grain increment when the doping concentration is increasing and these result also exactly related to the crystalline size of the calcined powders from the XRD pattern. Due to surface volume ratio of the calcined powder reduces the melting temperature and increasing the grain size at the time of sintering. But in the undoped (x=0) $BaTiO_3$ having high grain and well sintered. The sintered pellets were coated with platinum thin layer in automatic sputtered coating for SEM study. Fig.17 shows the EDX spectra of $Ba_{1-x}Bi_{2x/3}TiO_3$ ceramic, in EDX spectra it is clearly seen that the prepare $Ba_{1-x}Bi_{2x/3}TiO_3$ ceramic compound is only composition of Ba, Bi, Ti, and O. It gives the weight percentage and atomic percentage of the compound. Little amount of Bismuth is modifying the whole part of the crystal symmetry. Table.4 Weight % and Atomic % of all elements present in the $Ba_{1-x}Bi_{2x/3}TiO_3$ pellets.

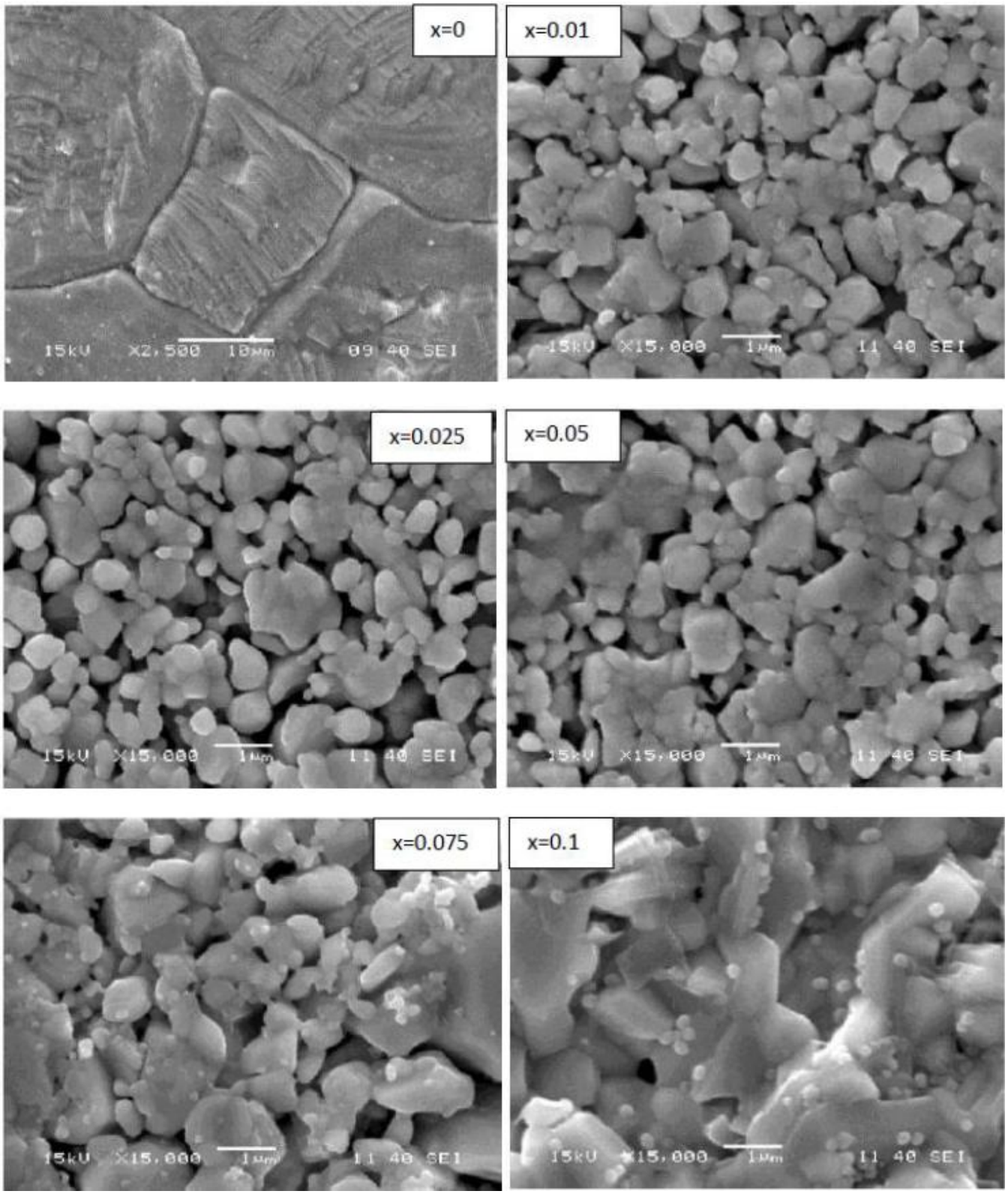

(**Fig.16** SEM picture of $Ba_{1-x}Bi_{2x/3}TiO_3$ pellets for all composition of x)

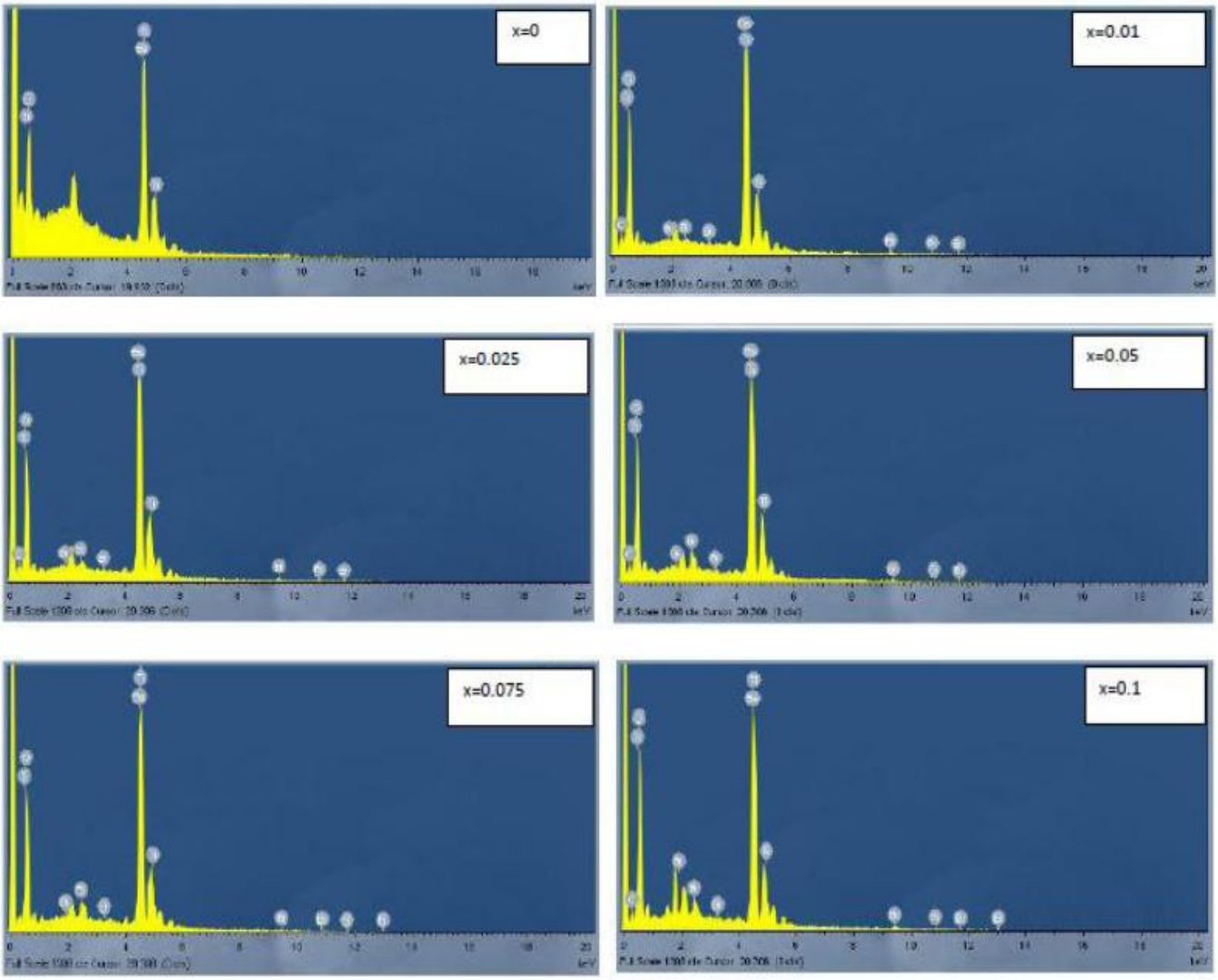

(Fig.17 EDX spectrum of $Ba_{1-x}Bi_{2x/3}TiO_3$ pellets**)**

Table 4 Weight % and Atomic % of all elements present in the $Ba_{1-x}Bi_{2x/3}TiO_3$ pellets

Element	Weight%	Atomic%	Weight%	Atomic%	Weight%	Atomic%	Weight%	Atomic%	Weight%	Atomic%	Weight%	Atomic%
	X = 0		X= 0.01		X= 0.025		X= 0.05		X= 0.075		X= 0.1	
O K	17.10	57.43	19.77	55.24	22.36	59.14	19.54	61.21	21.81	57.21	25.34	61.84
Ti K	13.89	15.58	14.26	14.75	15.62	14.79	14.75	15.43	14.75	14.22	14.08	12.49
Ba L	69.01	27.00	64.31	22.90	61.11	20.19	60.76	22.17	59.23	19.92	58.08	17.96
Bi M	---	---	1.66	0.39	0.91	0.20	4.94	1.19	4.19	0.93	2.50	17.96
Total	100		100		100		100		100		100	

4.3 Dielectric

In Fig.18 shows the Relative permittivity of sintered pellets of $Ba_{1-x}Bi_{2x/3}TiO_3$ for x= 0, 0.025 and 0.05. The sintered samples were coated with silver paste on both sides and heated at 500°C for 30 minutes for perfect conductivity of the electrodes. The permittivity at 1 kHz as a function of temperature for $Ba_{1-x}Bi_{2x/3}TiO_3$ ceramics under different concentration of x= 0, 0.025 & 0.05.

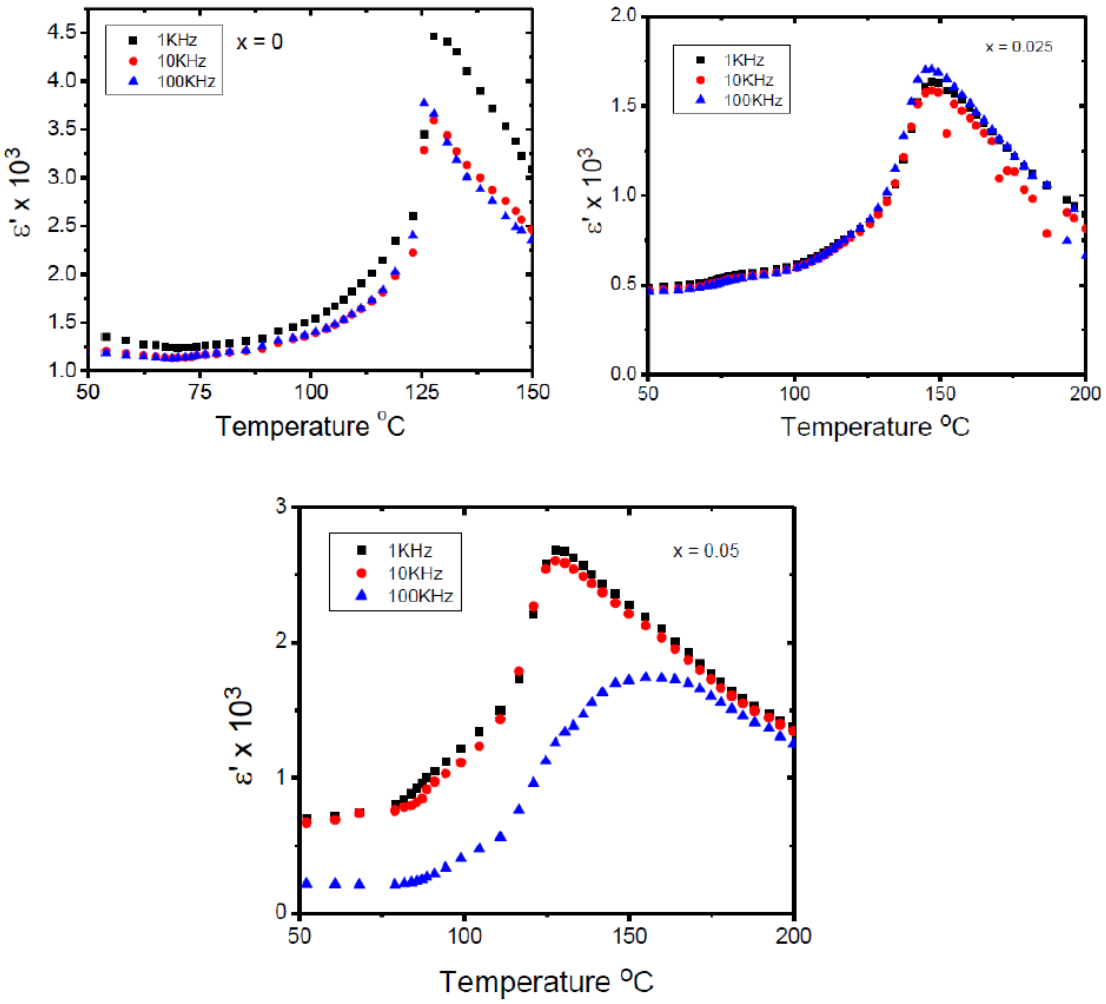

(Fig.18 Relative permittivity Vs Temperature of sintered pellets of $Ba_{1-x}Bi_{2x/3}TiO_3$ for x= 0, 0.025 and 0.05**)**

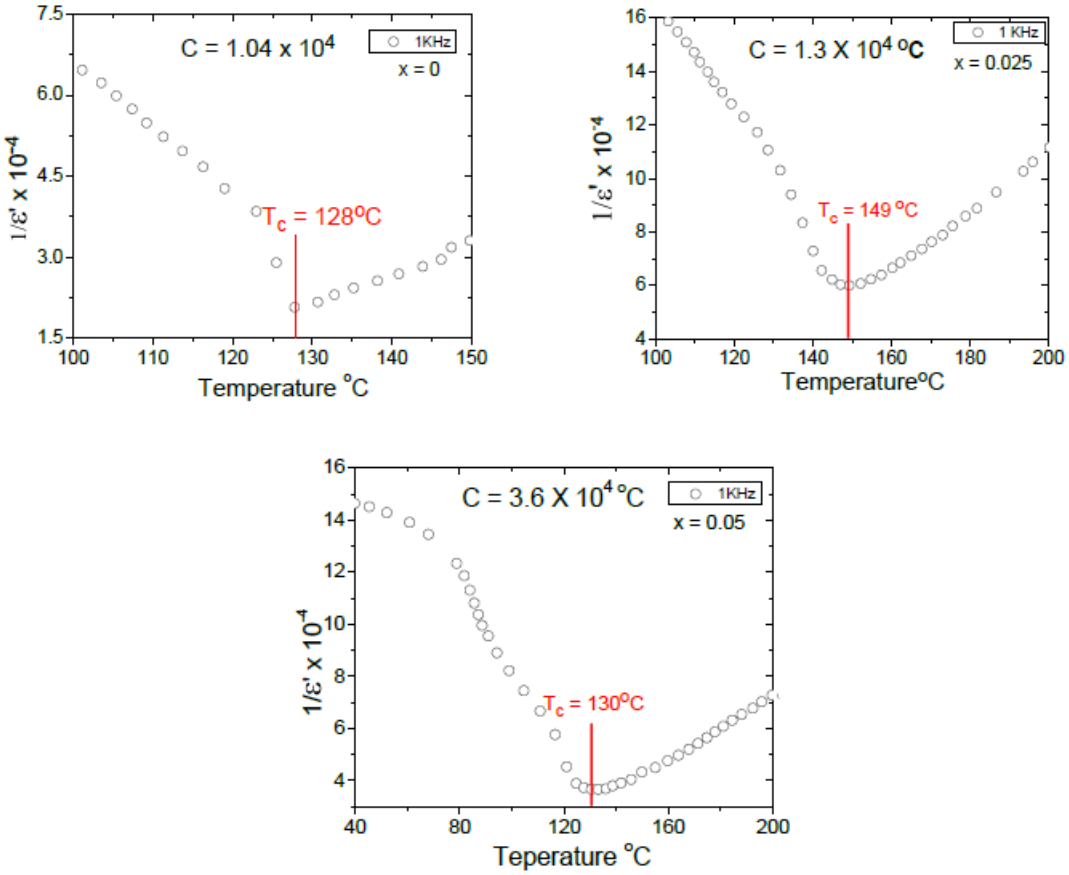

(Fig.19 Inverse relative permittivity with temperature**)**

In the relative permittivity versus temperature plots of x=0, 0.025 and 0.05 samples displayed sharp peaks at a transition temperature of around 140°C. The $Ba_{1-x}Bi_{2x/3}TiO_3$ ceramics exhibited a decrease in the transition temperature with increased concentration of Bi_2O_3. The results showed an increase in permittivity up to a maximum for the composition of x = 0 is 4455 at transition temperature 128°C, for the composition x = 0.025 is 1635 at transition temperature 149°C and for composition x = 0.05 the maximum relative permittivity is 2674 at transition temperature 133°C.

In most ferroelectrics, the temperature dependence of the relative permittivity above the Curie temperature (in paraelectric phase regime) can be described accurately by a simple relationship called the Curie-Weiss law.

$$\varepsilon = \varepsilon_0 + \frac{C}{T - T_0}$$

where C is the Curie-Weiss constant and T_0 the Curie- Weiss temperature. Generally, in the case of a first-order phase transition, $T_o<T_c$, while for the second-order phase transition $T_o=T_c$. Fig.19 shows the variation of inverse relative permittivity with temperature in the vicinity of transition temperature for $Ba_{1-x}Bi_{2x/3}TiO_3$ ceramics sintered at 1300 ^oC. The dielectric data show clearly first-order phase transition and excellent Curie-Weiss behavior. The Curie constant (C) obtained for this sample composition x = 0, 0.025, and 0.05 is $1.04x10^4$ ^oC, $1.3x10^4$ ^oC, and $3.6x10^4$ ^oC respectively, which is in good agreement with the reported value of pure BaTiO3.

CHAPTER-5
CONCLUSION

The $Ba_{1-x}Bi_{2x/3}TiO_3$ ceramic was prepared by the Solid state reaction method. XRD patterns showed that this material crystallizes in a perovskite-type single phase tetragonal structure with space group P4mm. SEM image shows the grain size decreases for x=0.01 and x=0.025 and increases with further addition of Bi concentration. The chemical composition of sintered pellets is analyzed by EDX. The temperature dependency dielectric study of $Ba_{1-x}Bi_{2x/3}TiO_3$ (i.e., x = 0, 0.025, 0.05) composition is studied. Dielectric constant and transition temperature decreases for x=0.025 and again increases for x=0.05. Curie constant values are calculated from the Curie Weiss law.

REFERENCES:

1. Henning D, Schnell A, and Simon G, *J Am. Ceram Soc*, 65 (1982) 539-544.
2. Yu Z, Guo R , Bhalla A S, *J.appl. Phys*, 88 (2000) 410.
3. Yu Z, Ang C, Guo R, Bhalla A S, *Appl. Phys. Lett*, 81 (2002) 1285.
4. Sciau Ph, Calvarin G, Ravez *J Solis State Communications*, 113 (2000) 77-82.
5. Wu T B, Wu C M and Chen M L, *Appl Phys Lett*, 69 (18) (1996) 2659,
6. Abe K, and Komatsu S, *J.appl. Phys*, 77 (1995) 6461.
7. Lu S G, Zhu X H, Mak C L, Wong K H, Chan H L W, and Choy C L, *Appl Phys Lett*. 82 (2003) 2877.
8. Zhu X H, Chong N, Lai-Wah Chan H, Mak C L, Wong K H, Liu Z G, and Ming N B, *Appl Phys Lett* 80 (2002) 3376.
9. Wang C, Cheng B L, wang S Y, Lu H B, Zhou Y L, Chen Z H, Yang G Z, *Appl Phys Lett*, 84 (5) (2004) 765.
10. "Elements of x-ray diffraction" Cullity B D, 2nd Edition, Addison- Wesley Publishing company, Inc.
11. Wong T K Y, Kennedy B J, Howard C J, Hunter B A, Vogt T , *J Solid State Chemistry*, **156**, 255 (2001).
12. Astala R K and Bristowe P D, *Modelling Simul. Mater. Sci Eng* 12 (2004) 79-90.
13. R. Pepinsky, Y. Okaya and F. Unterleitner, Acta. Cryst., **13**, 1071 (1960).
14. L. E. Cross, Ferroelectrics, **76**, 241 (1987).
15. N. Vittayakorn et. al. "Dielectric Properties of Bismuth Doped Barium Titanate ($BaTiO_3$) Ceramics" *Journal of Applied Science Research* **12** 1319 (2006).
16. M. R. Panigrahi et. al. "Synthesis and microstructure of Ca-dopedBaTiO3 ceramics prepared by high-energy ball-milling", *Physica B.* **404,** 4267 (2009).
17. M. R. Panigrahi et. al. "Structural analysis of100% relative intense peakof $Ba_{1-x}Ca_xTiO_3$ ceramics by X-ray powder diffraction method", *Physics B.* **405,** 1787 (2010).
18. Andrew J. Bell et. al. "Ferroelectrics: The role of ceramic science and engineering", *Journal of the European Ceramic Society*. **28,** 1307 (2008).
19. S. ZHANG et. al. "Normal ferroelectric to ferroelectric relaxor conversion in fluorinated polymers and the relaxor dynamics", *J. Materials Science*. **41,** 271 (2006).
20. N. Abdelmoula et. al. "Relaxor or classical ferroelectric behavior in A-site substituted perovskite type $Ba_{1-x}(Sm_{0.5}Na_{0.5})_xTiO_3$", *Solid State Sciences*. **8,** 880 (2006).
21. P. Kumar et. al. "Synthesis and dielectric properties of substituted barium titanate ceramics", *Journal of Alloys and Compounds*. **489,** 59 (2010).

22. N. Kumada et. al. “Rising Tc in Bi and Cu co-doped BaTiO3”, *Materials Letters.* **64,** 383 (2010).
23. W. Kugler et. al. “X-RAY DIFFRACTION ANALYSIS IN THE FORENSIC SCIENCE: THE LAST RESORT IN MANY CRIMINAL CASES”, *Advances in X-ray Analysis.* **46,** (2003).
24. S. Kumar et. al. “Relaxor behavior of BaBi4Ti3Fe0.5Nb0.5O15 ceramics”, Solid State Communications. **147**, 457 (2008).
25. T. Badapanda et. al. “Structural and dielectric relaxor properties of yttrium-doped $Ba(Zr_{0.25}Ti_{0.75})O_3$ ceramics", *Materials Chemistry and Physics.* **121,** 147 (2010).
26. T. Badapanda et. al. “Relaxor behavior of $(Ba_{0.5}Sr_{0.5})(Ti_{0.6}Zr_{0.4})O_3$ ceramics”, *Bull. Mater. Sci*., Vol. 31, No. **6,** 897 (2008).
27. S.K. Rout et. al. “Photoluminescence property of Ba(Zr0:25Ti0:75)O3 powder sprepared by solid state reaction and polymeric precursor method”, Physica B. **404,** 3341 (2009).
28. A. Al-Shahrani et. al. “Positive temperature coefficient in Ho-doped BaTiO3 ceramics”, Journal of Physics and Chemistry of Solids. **61,** 955 (2000).